Cell Reports, Volume *38*

Supplemental information

SCP4-STK35/PDIK1L complex is a dual phospho-catalytic signaling dependency in acute myeloid leukemia

Sofya A. Polyanskaya, Rosamaria Y. Moreno, Bin Lu, Ruopeng Feng, Yu Yao, Seema Irani, Olaf Klingbeil, Zhaolin Yang, Yiliang Wei, Osama E. Demerdash, Lukas A. Benjamin, Mitchell J. Weiss, Yan Jessie Zhang, and Christopher R. Vakoc

Figure S1. Phosphatase domain-focused CRISPR screening identifies context-specific dependencies in human cancer cell lines. Related to Figure 1.

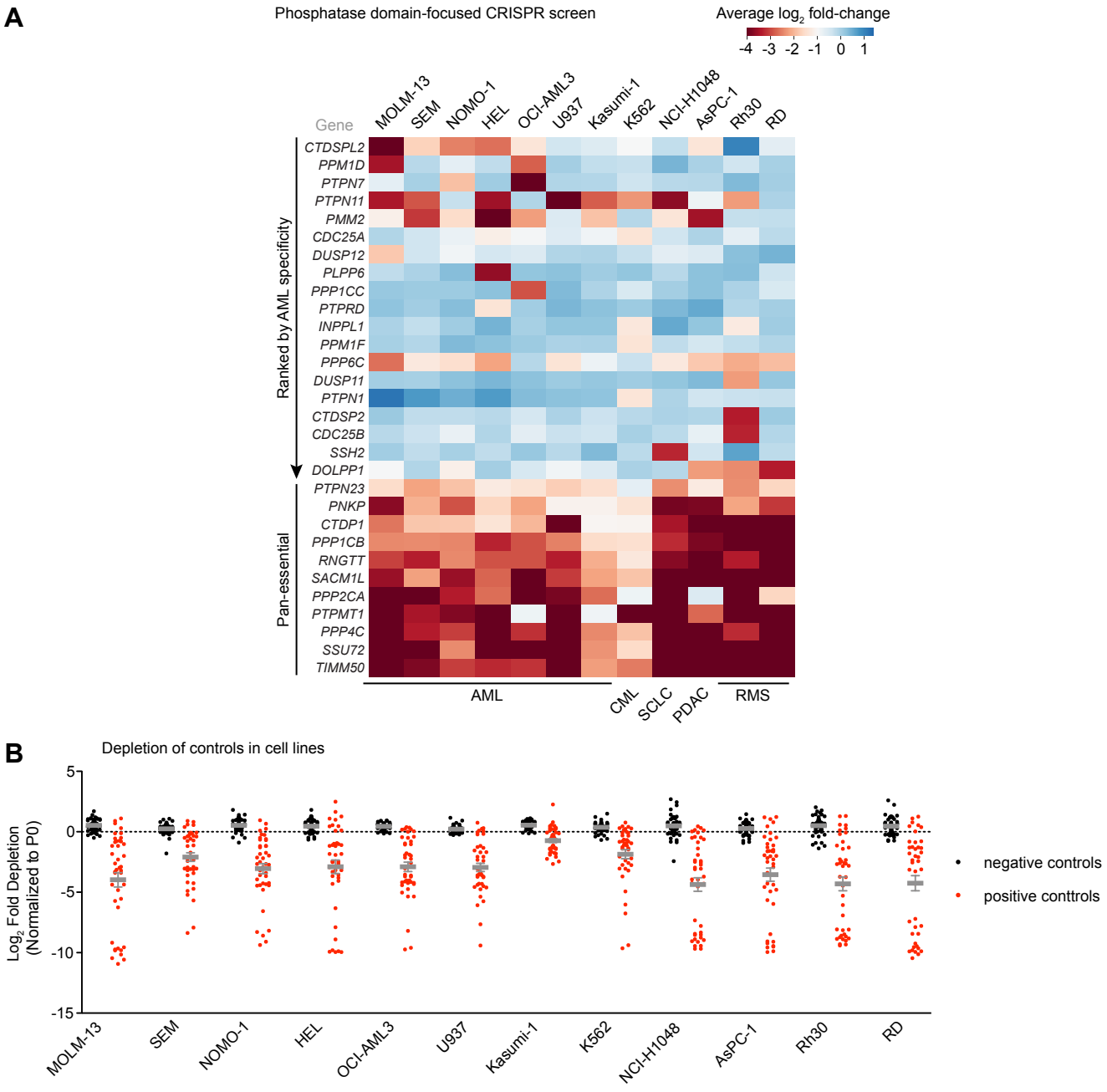

Figure S1. Phosphatase domain-focused CRISPR screening identifies context-specific dependencies in human cancer cell lines. Related to Figure 1.

(A) Extracted essentiality scores for phosphatases demonstrating AML-bias or pan-essentiality. Plotted is the $\log_2$ fold-change of sgRNA abundance during ~11 population doublings. The effects of individual sgRNAs targeting each domain were averaged. AML, acute myeloid leukemia; CML, chronic myeloid leukemia; SCLC, small cell lung cancer; PDAC, pancreatic ductal adenocarcinoma; RMS, rhabdomyosarcoma. **(B)** The $\log_2$ fold-changes of individual sgRNAs serving as negative (black) or positive (red) controls in the screen. **(C–E)** Extracted essentiality scores for selected phosphatases. Plotted is the $\log_2$ fold-change of sgRNA abundance during ~11 population doublings. The effects of individual sgRNAs targeting each domain were averaged. Also shown is the relevant oncogene/tumor suppressor status for each cell line.

Figure S2. SCP4 is an acquired dependency in human AML. Related to Figure 2.

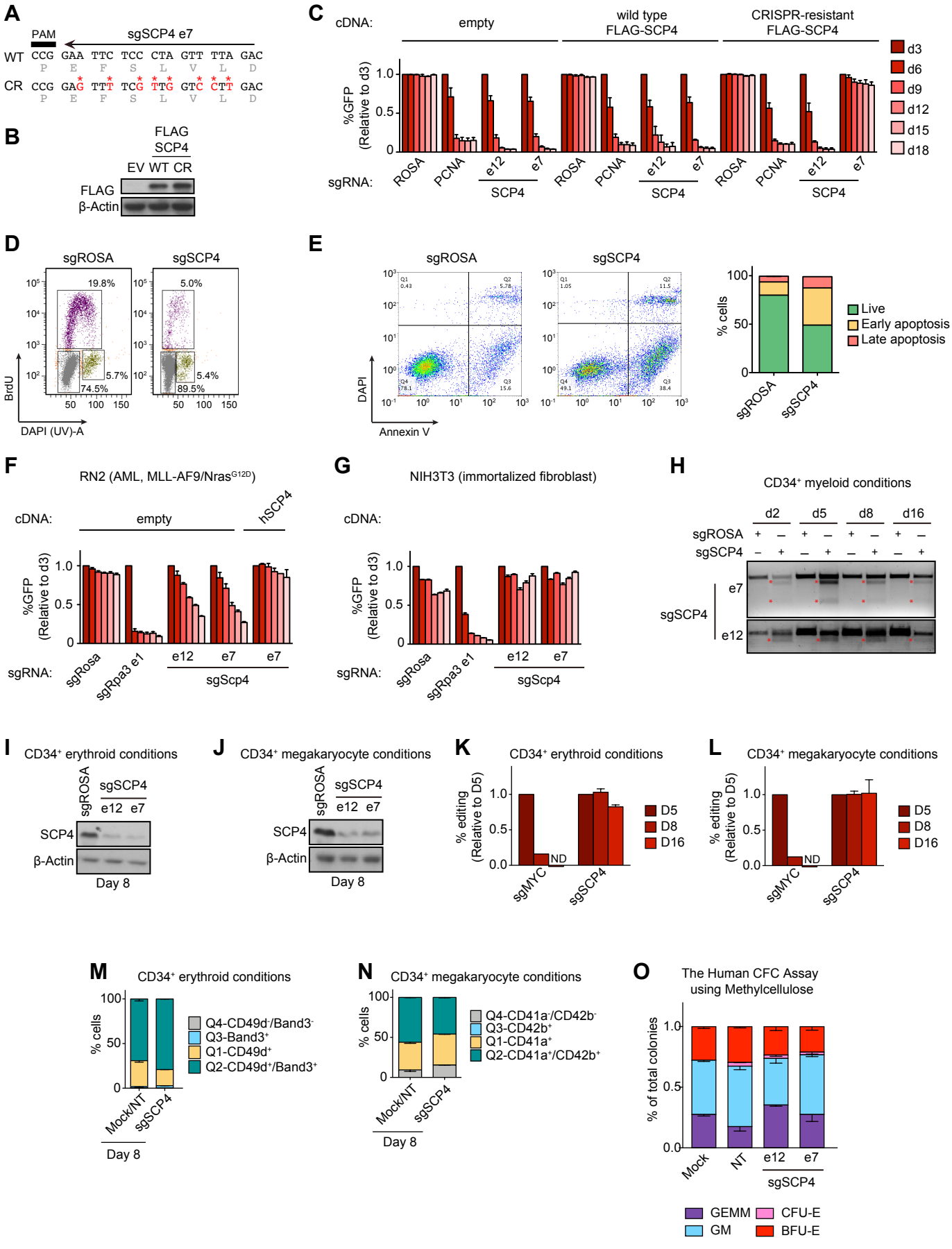

Figure S2. SCP4 is an acquired dependency in human AML. Related to Figure 2.

(A) Design of CRISPR-resistant mutant of SCP4. **(B)** Western blot of whole-cell lysates from MOLM-13 cells stably expressing empty vector (EV), wild type (WT), or CRISPR-resistant (CR) FLAG-SCP4. **(C)** Competition-based proliferation assay in MOLM-13 cells stably expressing empty vector, wild type, or CRISPR-resistant FLAG-SCP4 infected with the indicated sgRNAs. n = 3. **(D)** Representative flow cytometry analysis of BrdU incorporation and DNA content to infer cell cycle stage in MOLM-13 cells on day 5 post-infection with the indicated sgRNAs. **(E)** (Left) Representative flow cytometry analysis of DAPI (indicating permeable dead cells) and annexin-V staining (a pre-apoptotic cell marker) in MOLM-13 cells on day 5 post-infection with the indicated sgRNAs. (Right) Quantification of live and apoptotic cells. n = 3. **(F–G)** Competition-based proliferation assays in the murine cell lines infected with the indicated sgRNAs. Rescue in the RN2 cells stably expressing human SCP4 is shown. n=3. **(H)** Surveyor Assay analysis of indels presence during in $CD34^+$ cells electroporated with Cas9 loaded with the indicated sgRNAs over the course of culturing in myeloid conditions. **(I–J)** Western blot of whole-cell lysates from $CD34^+$ cells electroporated with Cas9 loaded with the indicated sgRNAs, day 8 post-electroporation in erythroid (I) and megakaryocyte (J) conditions. **(K–L)** RT-qPCR analysis of indels presence in $CD34^+$ cells electroporated with Cas9 loaded with the indicated sgRNAs over the course of culturing in erythroid (K) and megakaryocyte (L) conditions. The effects of individual sgRNAs for SCP4 were averaged. n = 4. **(M–N)** Quantification of the flow cytometry analysis of erythroid (M) and megakaryocyte (N) differentiation of $CD34^+$ cells electroporated with Cas9 loaded with the indicated sgRNAs, day 8 post-electroporation, culturing in erythroid (M) and megakaryocyte (N) conditions. The effects of individual negative controls and sgRNAs for SCP4 were averaged. n = 4. **(O)** The Human Colony Forming Cell (CFC) assay using methylcellulose. GEMM, colony forming unit-granulocyte, erythrocyte, macrophage, megakaryocyte; GM, colony forming unit-granulocyte, macrophage; CFU-E, colony forming unit-erythroid; BFU-E, burst forming unit-erythroid.

All bar graphs represent the mean ± SEM. All sgRNA experiments were performed in Cas9-expressing cell lines. ‘e’ refers to the exon number targeted by each sgRNA. The indicated sgRNAs were linked to GFP. GFP^+ population depletion indicates loss of cell fitness caused by Cas9/sgRNA-mediated genetic mutations. ROSA, Mock, and NT, negative controls; PCNA, Rpa3, and MYC, positive controls.

Figure S3. The catalytic phosphatase function of SCP4 is essential in AML. Related to Figure 3.

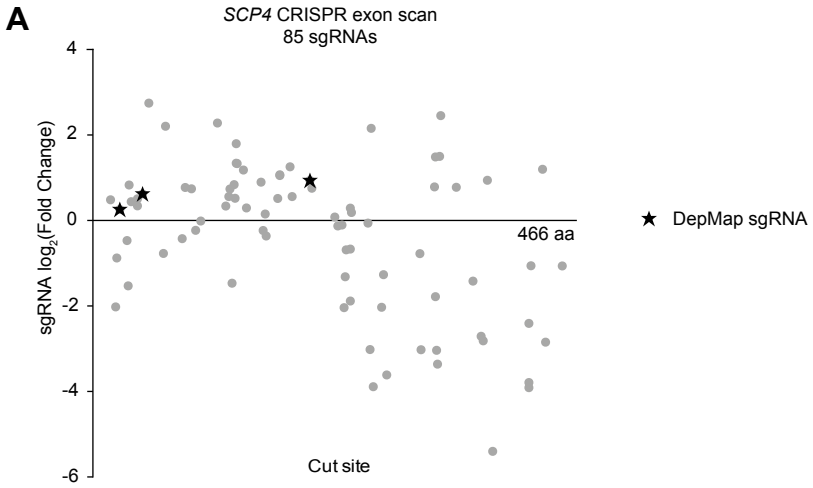

Figure S3. The catalytic phosphatase function of SCP4 is essential in AML. Related to Figure 3. **(A)** The CRISPR-scan of SCP4 with all the possible sgRNAs. Deep sequencing-based measurement of the impact of 85 SCP4 sgRNAs on the proliferation of MOLM-13 cells.

Figure S4. SCP4 directly interacts with two kinase homologs STK35 and PDIK1L. Related to Figure 4.

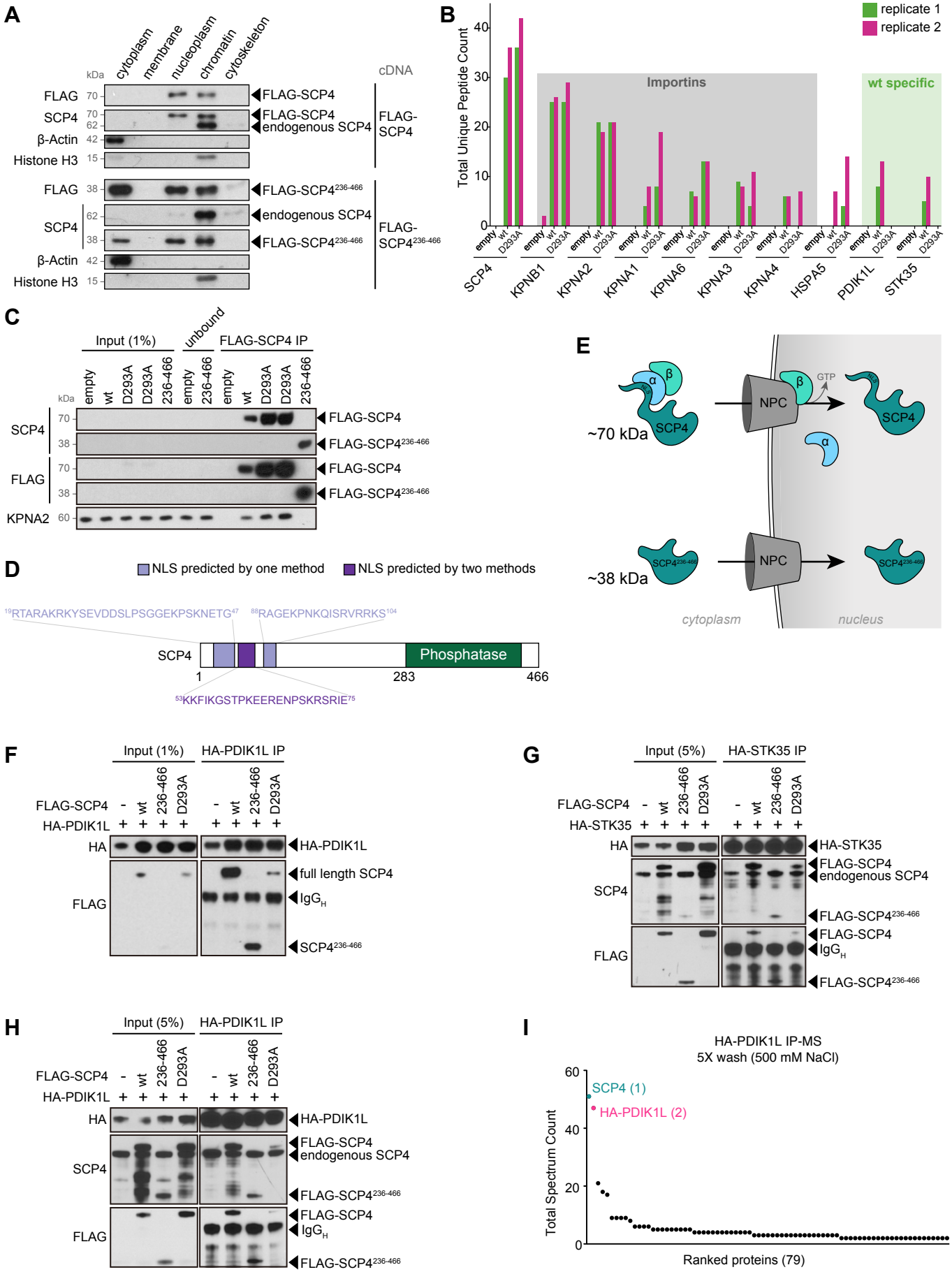

Figure S4. SCP4 directly interacts with two kinase homologs STK35 and PDIK1L. Related to Figure 4.

(A) Western blot of the indicated fractions from MOLM-13 cells stably expressing FLAG-SCP4^{WT} and FLAG-SCP4$^{236-466}$. **(B)** Total unique peptide counts for the top hits detected by MS in two independent biological replicates. **(C)** Immunoprecipitation followed by Western blotting performed with the indicated antibodies. The nuclear lysates were prepared from the human MOLM-13 cells stably expressing empty vector, FLAG-SCP4^{WT}, FLAG-SCP4$^{236-466}$, catalytic mutant FLAG-SCP4^{D293A}. The flow-through was analyzed to ensure efficient binding of the FLAG-tagged constructs (loaded as "unbound"). **(D)** Nuclear localization signals (NLS) predictions for SCP4 amino acid sequence performed by two different methods (Nguyen Ba et al., 2009; Kosugi et al., 2009). **(E)** Model of full length and truncated SCP4 transport into the nucleus. **(F–H)** Immunoprecipitation followed by Western blotting performed with the indicated antibodies. The whole-cell lysate was prepared from HEK293T 24 hours post-transfection with the indicated constructs (F). The nuclear lysates were prepared from the human AML cell line MOLM-13 stably expressing the indicated constructs (G, H). '-', empty vector; WT, wild type FLAG-SCP4; 236-466, FLAG-SCP4$^{236-466}$; D293A, catalytic mutant FLAG-SCP4^{D293A}, IP, immunoprecipitation. Note: degradation bands appear in the WT and D293A input at ~50 kDa and at ~40 kDa and the WT IP at ~40 kDa. **(I)** Total spectrum counts (TSC) for HA-PDIK1L and endogenous SCP4 detected by mass spectrometry on Pierce Anti-HA Magnetic Beads after stringent washes with washing buffers containing 500 mM NaCl.

Figure S5. STK35 and PDIK1L function redundantly in the same genetic pathway as SCP4. Related to Figure 5.

A

Clinical characteristic		*CTDSPL2*^{high} (n=35)	*CTDSPL2*^{low} (n=35)	*p* value
Gender		23:12 M:F	16:19 M:F	ns
Age (years)		51 (range 22-77)	60 (range 30-81)	ns
FAB subtype	**M0**	**9 (25.71%)**	**0**	**0.0022**
	M1	7	7	ns
	M2	8	6	ns
	M3	2	3	ns
	M4	8	6	ns
	M5	**0**	**13 (37.14%)**	**0.0001**
	M6	0	0	ns
	M7	0	0	ns
	nc	1	0	ns

B

Clinical characteristic		*PDIK1L*^{high} (n=35)	*PDIK1L*^{low} (n=35)	*p* value
Gender		21:14 M:F	18:17 M:F	ns
Age (years)		56 (range 22-77)	61 (range 22-88)	ns
FAB subtype	**M0**	**10 (28.57%)**	**0**	**0.0009**
	M1	8	6	ns
	M2	11	7	ns
	M3	1	2	ns
	M4	1	6	ns
	M5	**0**	**13 (37.14%)**	**0.0001**
	M6	1	0	ns
	M7	3	0	ns
	nc	0	1	ns

C

Clinical characteristic		*STK35*^{high} (n=35)	*STK35*^{low} (n=35)	*p* value
Gender		18:17 M:F	17:18 M:F	ns
Age (years)		60 (range 21-76)	57 (range 22-77)	ns
FAB subtype	M0	2	5	ns
	M1	**13 (37.14%)**	**4 (11.43%)**	**0.024**
	M2	7	8	ns
	M3	2	4	ns
	M4	3 (8.57%)	10 (28.57%)	0.0624
	M5	4	3	ns
	M6	1	0	ns
	M7	2	0	ns
	nc	1	1	ns

Figure S5. STK35 and PDIK1L function redundantly in the same genetic pathway as SCP4. Related to Figure 5.

RNA seq V2 data was obtained for the 173 AML patient samples in the TCGA database. RSEM values were used to select patients with the relatively high and low expression of (A) SCP4, (B) PDIK1L, and (C) STK35. Top and bottom 20% (35 patients) were selected respectively. Fisher's exact test was used to calculate the *p* values. ns: not significant.

Figure S6. SCP4 functions upstream of STK35/PDIK1L to support AML proliferation. Related to Figure 6.

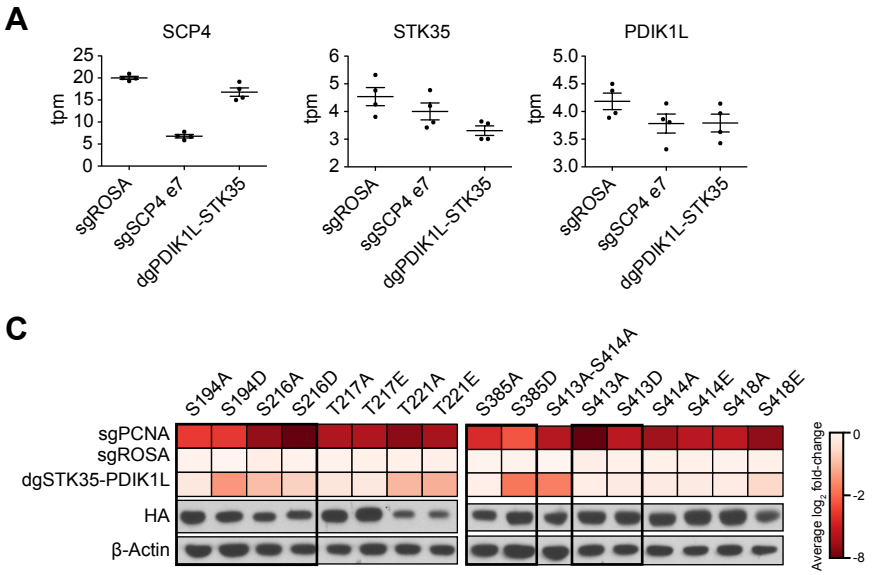

Figure S6. SCP4 functions upstream of STK35/PDIK1L to support AML proliferation. Related to Figure 6.

(A) RNA-Seq transcripts per million (tpm) data for SCP4, STK35, and PDIK1L from MOLM-13 cells on day 5 post-infection with the indicated sgRNAs. Plotted are data from each individual RNA-Seq replicate, the mean ± SEM. **(B)** Western blot of cytoplasm (Cyto) and nucleus (Nucl) fractions of MOLM-13 cells on day 5 post-infection with the indicated sgRNAs. STK35/PDIK1L simultaneous depletion was assessed by the loss of fitness during 18 days in culture showed in Figure 5A. **(C)** Summary of competition-based proliferation assays in MOLM-13 cells stably expressing CRISPR-resistant HA-PDIK1L or HA-STK35 constructs harboring the indicated amino acid substitutions infected with the indicated sgRNAs. Plotted is the fold change (log_2) of $sgRNA^+/GFP^+$ cells after 18 days in culture (average of triplicates). Below are shown Western blots of whole-cell lysates of the cells stably expressing the indicated constructs.

All sgRNA experiments were performed in Cas9-expressing cell lines. 'e' refers to the exon number targeted by each sgRNA. 'dg' refers to the bi-cistronic vector for simultaneous targeting of STK35 and PDIK1L. Negative fold-change indicates loss of cell fitness caused by Cas9/sgRNA-mediated genetic mutations.

Figure S7. SCP4-kinase complex supports metabolic homeostasis of AML cells. Related to Figure 7.

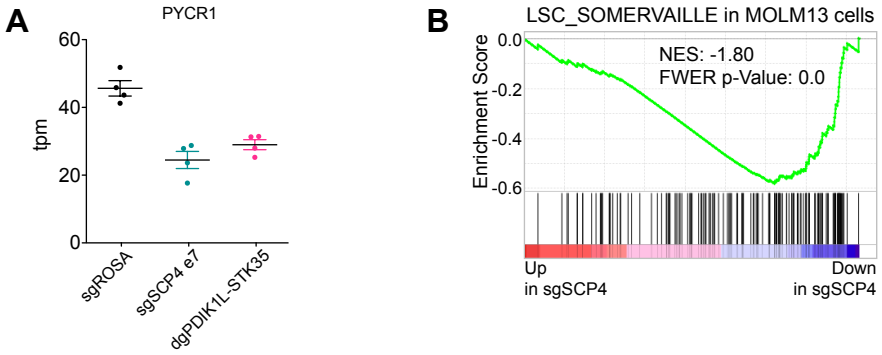

Figure S7. SCP4-kinase complex supports metabolic homeostasis of AML cells. Related to Figure 7.

(A) RNA-Seq transcripts per million (tpm) data for *PYCR1* from MOLM-13 cells on day 5 post-infection with the indicated sgRNAs. Plotted are data from each individual RNA-Seq replicate, the mean ± SEM. All sgRNA experiments were performed in Cas9-expressing cell lines. 'e' refers to the exon number targeted by each sgRNA. 'dg' refers to the bi-cistronic vector for simultaneous targeting of STK35 and PDIK1L. **(B)** GSEA plot of the LSC_SOMERVAILLE gene signature upon SCP4 knockout in MOLM13 cells.